P6.5 SENSITIVITY OF EAST COAST WINTER STORMS TO SEA SURFACE TEMPERATURE GRADIENTS

Neil A. Jacobs[1*], Sethu Raman[2], and Gary M. Lackmann[2]

[1]AirDat, LLC, Morrisville, North Carolina
[2]North Carolina State University, Raleigh, North Carolina

1. INTRODUCTION AND MOTIVATION

Mid-latitude cyclones, known as Nor'easters when they track northward along the East Coast of North America, have a long history of producing severe, and sometimes catastrophic, blizzard conditions along the eastern seaboard. The coastal region east of the Carolinas, in association with the warm Gulf Stream current, has been identified as an epicenter of extratropical cyclogenesis in previous climatological studies; this is due in part to the semi-permanent thermal gradient found along the western edge of the Gulf Stream. Extensive research has been done on the pre-storm marine boundary layer (MBL) baroclinicity and air-sea interactions associated with extratropical cyclones (e.g., Bosart et al. 1972; Sanders and Gyakum 1980; Kuo and Low-Nam 1990; Raman and Reddy 1996). Cione et al. (1993) show that the pre-storm baroclinicity, which includes the pre-storm Gulf Stream front (GSF) position, sea surface temperatures, and average coastal air temperatures, is correlated to the intensification of coastal cyclones. Results from the Cione et al. (1993) study reveal that the rate of surface cyclonic intensification is related to both the thermal structure of the continental airmass and the position of the GSF in relation to land. The influence of the Gulf Stream on the overlying atmosphere is a significant factor in determining the nature of the cyclogenesis process in this region. The Atlantic Surface Cyclone Intensification Index (ASCII) is a forecast index that quantifies the strength of low-level baroclinicity off the coast of the Carolinas during a cold-air outbreak. The pre-storm baroclinic index (PSBI) is obtained through a calculation of the gradient between the coldest 24-h average coastal air temperature (T) and the GSF temperature (T_{GSF}),

$$PSBI = \frac{T_{GSF} - T}{d}, \quad (1)$$

where d is the distance of the GSF from the coast (Cione et al. 1993). The PSBI value indicates the potential for rapid cyclogenesis, provided an upper-tropospheric disturbance is approaching the domain (Cione et al. 1993, their Fig.1), and can explain as much as 31% of the storm deepening rate variance (Cione et al. 1998). Jacobs et al. (2005) found that as much as 74% of the variance in deepening rate can be explained by the PSBI when the absolute vorticity of the upper-tropospheric disturbance is used to categorize extratropical cyclone events.

A two-part study is conducted on the sensitivity of lower-tropospheric cyclogenesis to the sea surface thermal gradient associated with the Gulf Stream. The first part (Part-1) is carried out by systematically reducing the magnitude of the sea surface temperature (SST) gradient by 50% for three consecutive mesoscale model simulations of the 24-25 January 2000 winter storm to verify the PSBI. This is done to test the hypothesis that numerical simulations of this case will follow deepening rates predicted by the PSBI. All other model initialization parameters are left unchanged with the exception of the SST file. In the second part (Part-2), the Gulf Stream is shifted to the east by 1° and 2.5° of longitude for two respective experimental numerical simulations, while leaving the unique features such as curvature of the Gulf Stream and the SST values unchanged. The objectives of Part-2 are to (i) isolate the contribution of surface-level forcing based on the position of the Gulf Stream without changing the magnitude of the SST, and (ii) to verify ASCII from the GSF position parameter, as well as to test the hypothesis that by altering the track of the surface low, the feedback link to the upper-level trough will be weakened, thus reducing the surface-level cyclogenesis.

2. 24-25 JANUARY 2000 CASE

Four days prior to the 24 January 2000 storm, an area of low pressure developed along the Carolina coast and tracked northeast off the mid-Atlantic United States. A high pressure system extended southeastward behind this first coastal low, and northwesterly winds advected a cold air mass off the coast of the Carolinas and over the Gulf Stream. The 24-h temperature observations beginning 1200 UTC Jan 20 decreased as much as 15°C in the coastal region between Wilmington, NC (station KILM) and Morehead City, NC (station CLKN7). This offshore flow remained in place for more than 48 h, and was followed by the development of a coastal front over the western edge of the Gulf Stream.

The surface low associated with the 24 January 2000 cyclone formed in the northern Gulf of Mexico, and began to track along this stationary coastal front northeast of Florida, and downstream from an upper-level trough. As it moved over the Gulf Stream from Charleston, SC to Cape Hatteras, NC, the pressure dropped at a rate in excess of 1.3 mb h^{-1}. The closed

*Corresponding author address: Neil A. Jacobs, AirDat, LLC, 2400 Perimeter Park Dr. Suite 100, Morrisville, NC 27560. Email: njacobs@airdat.com

circulation was located east of South Carolina at 0000 UTC on Jan 25, and moved northeast, parallel to the coast, following a frontal boundary that established along the temperature gradient formed by the western boundary of the Gulf Stream. The surface low continued to move north, and was located east of New England by 0000 UTC Jan 26. The winter storm brought heavy snowfall from the Carolinas through the New England region. Record snow amounts fell across central North Carolina with the Raleigh-Durham (RDU) airport reporting a snowfall accumulation of 20.3 in. (NCDC 2000a).

Prior to the explosive development, the NCEP Eta Model's 0000 UTC 24 January run failed to accurately predict not only the track, but the deepening rate and the precipitation amount for the event (e.g., Buizza and Chessa 2002; Zhang et al. 2002). Most operational forecasts exhibited an eastward bias in storm track, and forecasted less than 5 mm liquid equivalent precipitation for the RDU area. Additional studies have been conducted on this case in an attempt to understand the sources of forecast error (e.g., Langland et al. 2002; Brennan and Lackmann 2005). During this event, the GSF was less than 50 km off the shoreline of southeast NC. As a result, the pre-storm baroclinic index was estimated to be greater than $2°C\ 10^{-1}\ km^{-1}$ suggesting that rapid cyclogenesis was likely.

3. MODEL DESCRIPTION

The simulations in the following two-part study were conducted using version 3.6 of the fifth-generation Pennsylvania State University–National Center for Atmospheric Research (NCAR) Mesoscale Model (MM5; e.g., Dudhia 1993; Grell et al. 1994). A single 10-km domain with 38 vertical σ-levels was initialized at 0000 UTC 24 January 2000 with the National Centers for Environmental Prediction (NCEP) operational analysis from the Eta-212 (40-km) grid. The model forecast was run to 48 hours (0000 UTC 26 Jan). The Grell cumulus parameterization was chosen for its handling of convective precipitation at smaller grid scales. The Blackadar planetary boundary layer scheme was chosen because of its successful handling of winter storm systems when paired with the Grell cumulus parameterizations (Grell 1993). The other reason for employing the Grell/Blackadar combination was the use of the 5-layer soil model. Previous testing of various land surface models (LSM) for this case showed no significant differences. Sensitivity studies suggest that snow cover and the lack of vegetation during the winter months reduce the LSM's effect on the atmospheric surface layer (Chen and Dudhia 2001). This is understandably so for cases in the winter where the influence of vegetation is negligible. In fact, the northern most 30% of the domain for the 24 Jan 2000 case was initialized with snow covering the ground from the weekly snow cover analysis from the NCEP reanalysis (Ek et al. 2003; Kalnay et al. 1996).

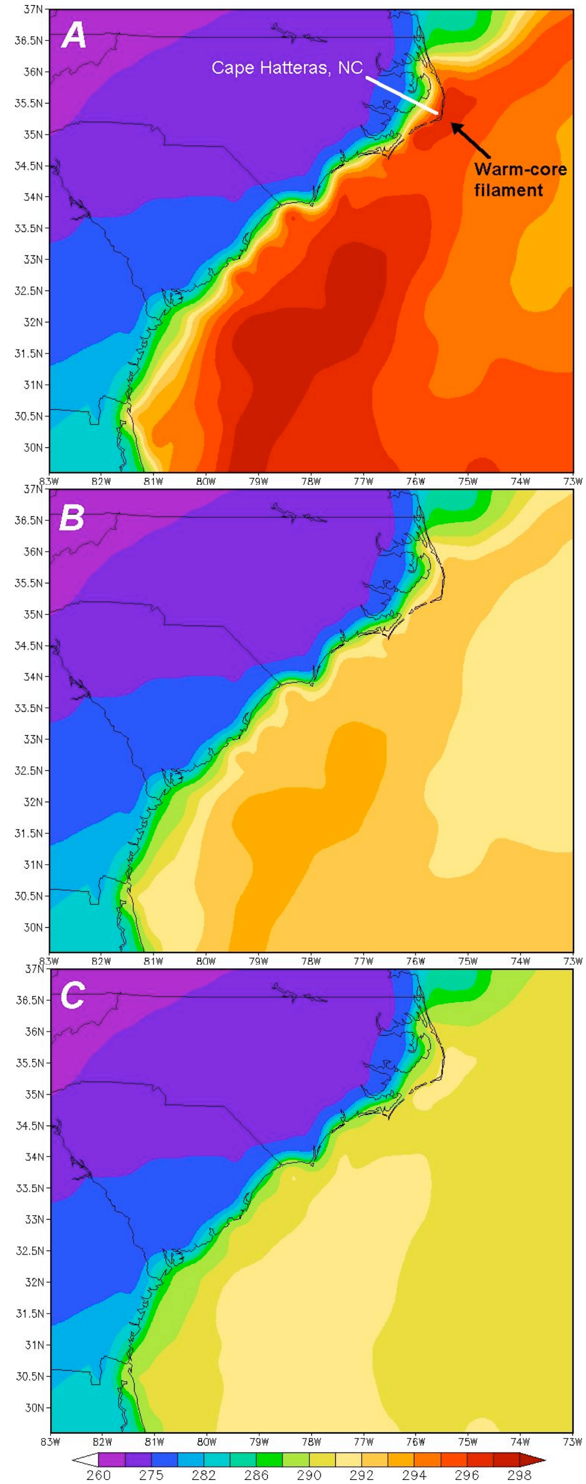

Fig. 1. The three SST input files used in the simulations where *Exp-A* is the SST file with the largest gradient, *Exp-B* is the product of the first smoothing run, and *Exp-C*, the weakest gradient, a product of the second smoothing run.

4. EXPERIMENT DESIGN: PART-1

Three different simulations, referred to as *Exp-A*, *Exp-B*, and *Exp-C*, were run in this experiment with the only change being the systematic damping of the SST initialization field. This was done beginning with the unchanged SST data file (Fig. 1a) used in *Exp-A*.

The SST data in simulation *Exp-A* was obtained from the NCEP operational analysis on the Eta-212 grid. The equation for the smoothing that simulations *Exp-B* and *Exp-C* underwent (Fig. 1b and 1c) is expressed as:

$$T = T_c + \frac{1}{2}\left(T_0 - T_c\right) \qquad (2)$$

where T is the calculated SST, T_c is the SST of the near coast (beach front), and T_0 is the initial SST. In order to only have this algorithm applied to the SST, and leave the land temperatures unchanged, a lower limit of 290 K was placed on T_c and T_0. This method changes the PSBI systematically; however, it changes the GSF-to-coast distance as well as the GSF temperature. Therefore, a separate dependence cannot be identified between the horizontal distance and the temperature of the GSF. However, the objective of this experiment is to verify ASCII using a mesoscale model simulation. Since the PSBI in (1) includes both parameters, whether the numerator is increased, or the denominator is decreased, yields the same PSBI values as seen by the ASCII regression fit forecast method. The post-smoothed SST input files can be seen in Fig. 1. Simulation *Exp-A* has the largest SST gradient, and simulation *Exp-C* has the smallest gradient. The deepening rate is defined by the largest 12-h pressure drop as the surface low passes through the ASCII domain, which is the same method employed by Cione et al. (1993) and Jacobs et al. (2005).

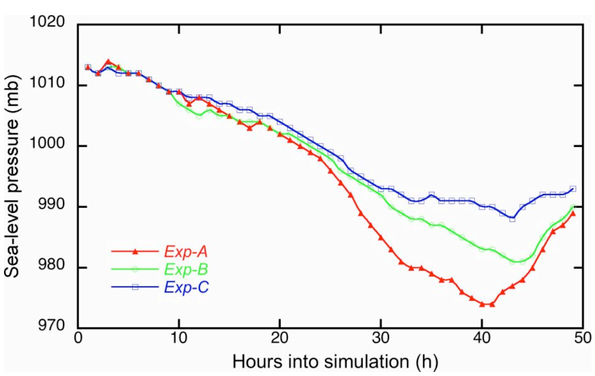

Fig. 2. Time series of the lowest central sea-level pressure for the *Exp-A* (red), *Exp-B* (green), and *Exp-C* (blue) simulations. The hours into the simulation run from hour 1 to hour 49, and correspond to 0000 UTC 24 Jan to 0000 UTC 26 Jan.

5. RESULTS: PART-1

a) Sea-level pressure comparison

The deepening rate, or change in sea-level pressure, is of most concern because of its use in the ASCII forecast. Between 0000 and 0900 UTC 25 Jan, the difference in position (not shown) between the *Exp-A* simulation and the other two simulations is > 100 km, where *Exp-A* is closer to the coast. At this time, the variance in sea-level pressure becomes quite evident (24 to 33 h; Fig. 2). By 0900 25 Jan (33 h into simulation), the positions of the central low pressures begin to converge towards the same track (Fig. 3). This is likely a result of the cyclones moving north of the region of SST gradient. However, the difference in sea-level pressure continues to grow, where *Exp-A* is 980 mb, *Exp-B* is 988 mb, and *Exp-C* is 991 mb. At this point, *Exp-A* is obviously a significantly stronger storm.

b) PSBI and ASCII comparison

The PSBI results were computed from the numerical gridded output files of the simulations using (1), and are accurate to within 5 km (half the grid space difference). T_l = 5.6°C was recorded during the initialization (24 h prior to development), and is the same for *Exp-A*, *Exp-B*, and *Exp-C*. For simulation *Exp-A*, T_{GSF} = 25°C, and *d* = 70 km, which results in a PSBI value of 2.8°C 10^{-1} km^{-1}. This PSBI value is much higher than the PSBI value of 2.1°C 10^{-1} km^{-1} calculated using actual observations. For simulation *Exp-B*, T_{GSF} = 20°C, and *d* = 80 km, which results in a PSBI value of 1.8°C 10^{-1} km^{-1}. Finally, for simulation *Exp-C*, T_{GSF} = 19°C, and *d* = 110 km, which results in a PSBI value of 1.2°C 10^{-1} km^{-1}.

The time series of sea-level pressure, shown in Fig. 2, was used to obtain the deepening rate as the storm in each simulation crossed the domain (Cione et al. 1993, their Fig.1)[1]. For simulation *Exp-A*, the change in pressure was -19 mb, the largest drop of the 3 simulations. Both *Exp-B* and *Exp-C* experienced pressure decreases of -12 mb and -8 mb, respectively. These values are plotted against the PSBI values, discussed above, in Fig. 4, as a comparison against the ASCII dataset (1980-2002) of cyclone's ΔP/12h vs. PSBI from the Jacobs et al. (2005) study. The "Storms" (blue) linear regression fit combines both sets of storms (1980-1990 and 1991-2002), while the sensitivity simulations *Exp-A* (red circle), *Exp-B* (green circle), and *Exp-C* (blue circle) with regression fit appear in red. Although there are only three data points to base the regression on, it aligns well with the fit for the ASCII data set. The very high correlation coefficient of 0.99 for the sensitivity simulations fit is a result of only having 3 data points. Even with 3 points, the simulations fall in a line that share a similar slope as the ASCII fit. Since the SST gradient was exponentially decreased in half, the *Exp-A* falls much further down the vertical axis than *Exp-B* or *Exp-C*.

---

[1] The cyclones in all 3 simulations crossed the domain within 1 h of each other.

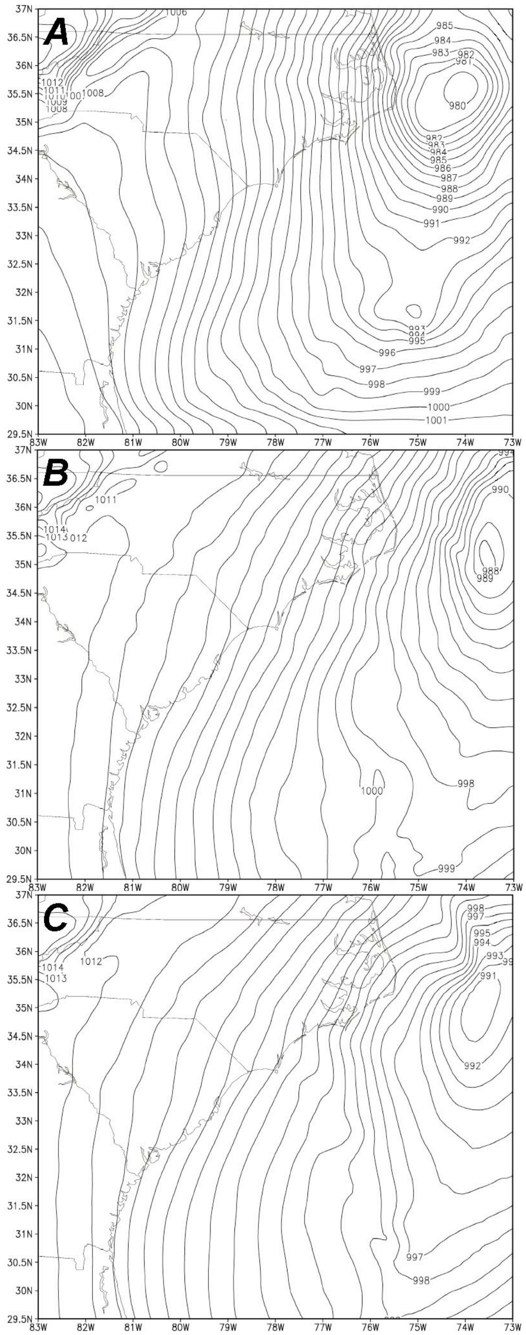

Fig. 3. Sea-level pressure for simulations *Exp-A*, *Exp-B*, and *Exp-C* valid 0900 UTC 25 Jan (33 h into simulation).

c) Discussion

The slope of the ASCII forecast regression fit is matched by the similar slope of the three simulations. Although these simulations share, for the most part[2], the same upper-level forcing characteristics, it turns out that the numerical values for this case are very close to the "average" for all the cases (1991-2002) thus placing the fit in the middle of the distribution. The PSBI for simulation *Exp-A* is unrealistic in a sense that using the "skin temperature" data placed the warm-core filament, seen in Fig. 1a, partly inside the Pamlico Sound (west of Cape Hatteras, NC), which is not physically possible. Not only are the SSTs excessively high, but there is essentially no transition from cold near-coast water to the GSF, as the GSF was placed along the coastline. However, the objective of this study is to have PSBI values that would separate the data points along the x-axis of the ASCII distribution, so unrealistically large, as well as small, PSBI values were intentionally derived.

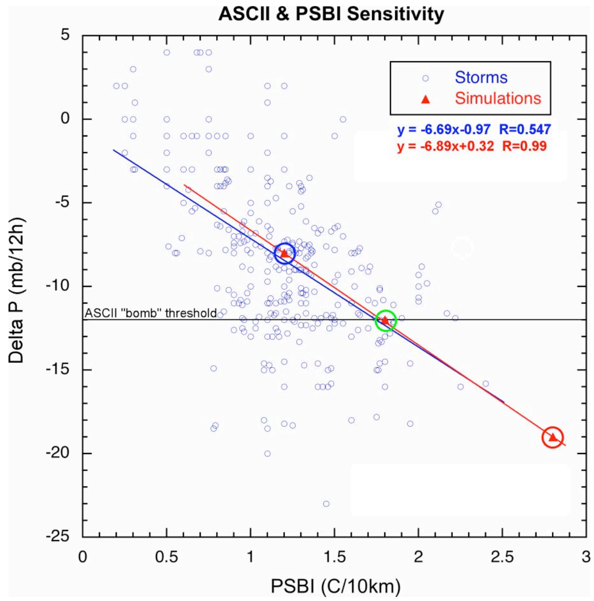

Fig. 4. The updated ASCII dataset (1980-2002) of cyclone's ΔP/12h vs. PSBI. The "Storms" (blue) linear regression fit, which combines both sets of storms (1980-1990 and 1991-2002), and the sensitivity simulations *Exp-A* (red), *Exp-B* (green), and *Exp-C* (blue) with regression fit (red).

The change in surface deepening rate did follow the trend forecasted by ASCII. Analysis of the individual simulations reveals a much deeper low pressure in *Exp-A* resulting from the vortex stretching and convergence along the frontal boundary that formed over the GSF connecting the southern branch to the warm-core filament (literally on Cape Hatteras). As a result, the cyclone in *Exp-A* took a more westerly track until north of the region where the GSF was more in line with *Exp-B* and *Exp-C*. Simulation *Exp-C* had the lowest PSBI, yet still continued to deepen to a rather large storm. Although there is still a significant

[2] All 3 simulations were initialized with identical atmospheric data; however, there exists an inherent inability to separate the upper-level forcing variance generated by the feedback from the surface low once the simulation is underway.

thermal gradient in *Exp-C* (compared to no gradient), most of the cyclogenesis was likely in response to the upper-level trough. As seen in Fig. 4, the three simulations align nicely with the ASCII regression fit, and offer a second method of verification to the original climatology, as well as further isolating the contribution of SST gradients to extratropical cyclogenesis.

6. EXPERIMENT DESIGN: PART-2

In Part-1 of this study, the 24-25 January 2000 winter storm was used to verify the PSBI by systematically damping the effects of the SST gradient. This was done to test the hypothesis that numerical simulations of this cyclone will follow deepening rates predicted by the PSBI. As expected, this was the case. However, there was an inherent inability to isolate which factor within the PSBI was responsible for rapid cyclogenesis (i.e., the Gulf Stream's position or Gulf Stream's SST) because the damping reduced the PSBI value as a whole. From (1), the resulting value could reflect either a smaller numerator (lower SST values), or larger denominator (greater distance from shore). The objective of Part-2 is to isolate the contribution to surface-level forcing based on the position of the Gulf Stream without changing the magnitude of the SST.

Three different simulations were run in this experiment with the only change being the SST initialization file. These simulations will be referred to as the control simulation (*Cntl*), the experimental-1 simulation (*Exp-1*), and the experimental-2 simulation (*Exp-2*). The *Exp-1* simulation shifted the high resolution grid of the Gulf Stream SST to the east by 1° of longitude, and the *Exp-2* simulation shifted the grid 2.5° of longitude to the east. The shifting of the Gulf Stream SST was the only change within the simulations. To create the SST field for the *Cntl* simulation, seen in Fig. 5, the 1.1-km high resolution data matrices were quilted over corresponding latitude and longitude grid coordinates of the Eta-212 SST. The 1.1-km SST data were derived from digital images acquired by the Advanced Very High Resolution Radiometer (AVHRR) carried onboard the NOAA-12 and NOAA-14 polar orbiting satellites, and obtained through NOAA's CoastWatch program (Li et al. 2002). The first step in the SST preprocessing was to obtain single pass 1.1-km resolution data sets by analyzing imagery preceding storm development with as little cloud cover as possible. The chosen imagery was from 22 January 2000, less than 2 days prior to the start of the simulations. This was early enough to reveal the dominant features of the Gulf Stream, but preceded the increase in cloud cover. This imagery was less than 10% corrupted with clouds. Preprocessing code developed at the State Climate Office of North Carolina was used to interpolate the remaining SST grid values where clouds were located. Ship and buoy observations were compared against the imagery in the data set to validate the SST off the southeast coast of NC. Once the cloud-free SST data set was constructed, it was mapped over the 10-km regridded analysis generated with the Eta-212 SST data set. This

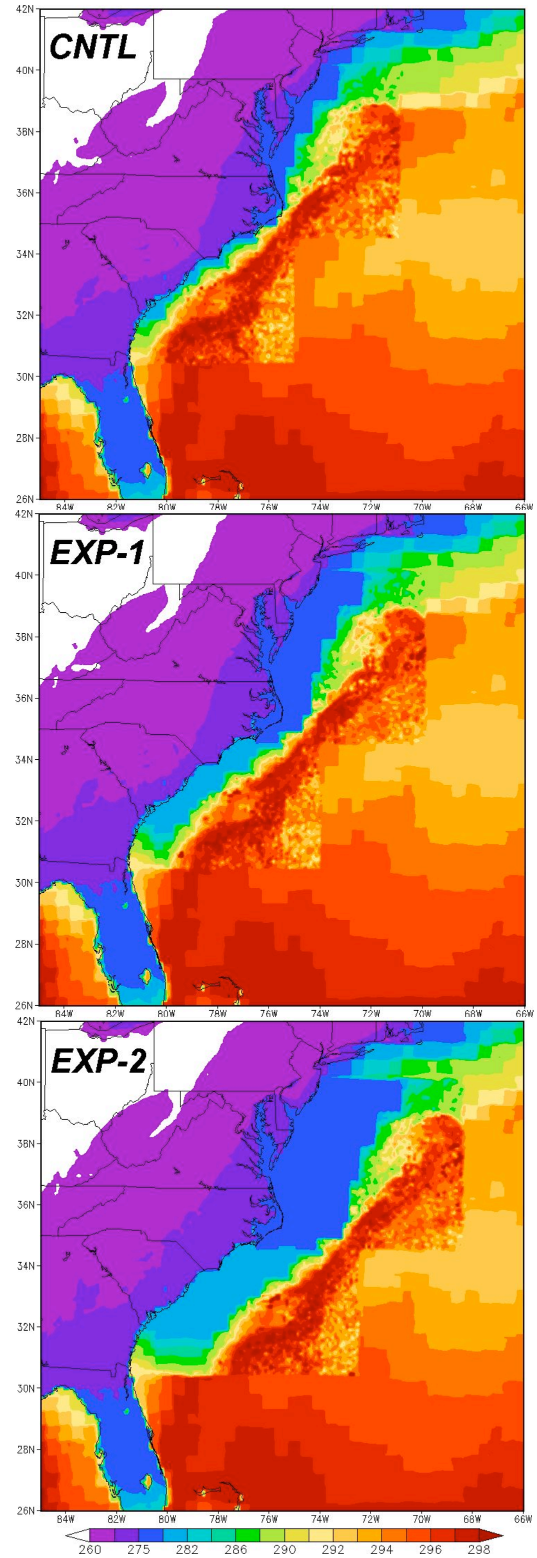

Fig. 5. The SST initialization files for the *Cntl* (no shift), *Exp-1* (1° of longitude shift), *and Exp-2* (2.5° of longitude shift) simulations post-regridded to 10 km. The high-resolution data is valid 22 Jan 2000.

was done beginning with the unchanged high resolution SST data file used in the *Cntl* (Fig. 5, CNTL). For *Exp-1* (Fig. 5, EXP-1) and *Exp-2* (Fig. 5, EXP-2), the Gulf Stream is shifted east along the x-axis (i.e., Δx varies with longitude) 1° and 2.5° of longitude, respectively. The Coastwatch 1.1-km data includes land and water temperatures, as well as offshore SST. As a result, the process of mapping these high resolution matrices shifted to the east would also map the warmer land temperatures over the ocean. To correct this, a script was written based on the land-sea mask of the grid file. After the boundary is defined, all grid points to the west along the x axis are adjusted to the same SST as the near-coastal waters. This results in the "step" transition of the SST values around 280 K seen in Fig 5.

Although this transition is of lower resolution than the adjacent 1.1 km GSF, it is still equal to, or higher than, the resolution of the remaining Eta-212 grid used in the background. Once the warmer inland values are changed to the temperature of the near-coastal waters, the matrices are mapped 1° to the east for *Exp-1* (Fig. 5, EXP-1), and 2.5° to the east for *Exp-2* (Fig. 5, EXP-2). These SST data sets are then used to initialize the respective simulations.

7. RESULTS: PART-2

a) Sea-level pressure comparison

Large variations in the evolution of the surface cyclone are not limited to location. The development of the precipitation shield from 0000 to 1800 UTC 25 Jan also reveals a temporal delay where the *Exp-1* simulation is lagging the *Cntl*, and the *Exp-2* simulation is lagging *Exp-1*. This horizontal displacement results in a temporal (~ 6 h), and spatial (~ 200 km NNE) offset of the precipitation from the *Cntl* to the *Exp-2* simulation between 0900 and 1500 UTC 25 Jan. Noticeable differences in the magnitude of precipitation can be seen in Fig. 6, which is valid 0900 UTC 25 Jan. This space-time lag is likely a result of the advecting of warm air at the surface-level being delayed from interacting with the upper-level trough because the source of the warm moist air has been shifted to the east for each consecutive experimental simulation.

Plots of 500-hPa divergence valid 0900 UTC 25 Jan are seen in Fig. 7. There is a strong correlation, as expected, between the upper-level divergence in Fig. 7 (blue arrow) and the precipitation seen in Fig. 6. Since only the SST fields were changed, variations in the upper-level flow between the simulations are a result of surface feedback. When comparing the sea-level pressure in Fig. 6, the difference in deepening rate is likely a factor of weakened feedback in the *Exp-1* and *Exp-2* simulations because the surface-to-upper-trough displacement was increased.

The lower-level response to the shift in the position of the Gulf Stream is most evident when observing the response from the 10-m winds between 2100 UTC 24 Jan and 0600 UTC 25 Jan (not shown). In the *Cntl* simulation, a well defined coastal front develops over the GSF along the 291 K isotherm. This convergence is also present in the 10-m winds of the

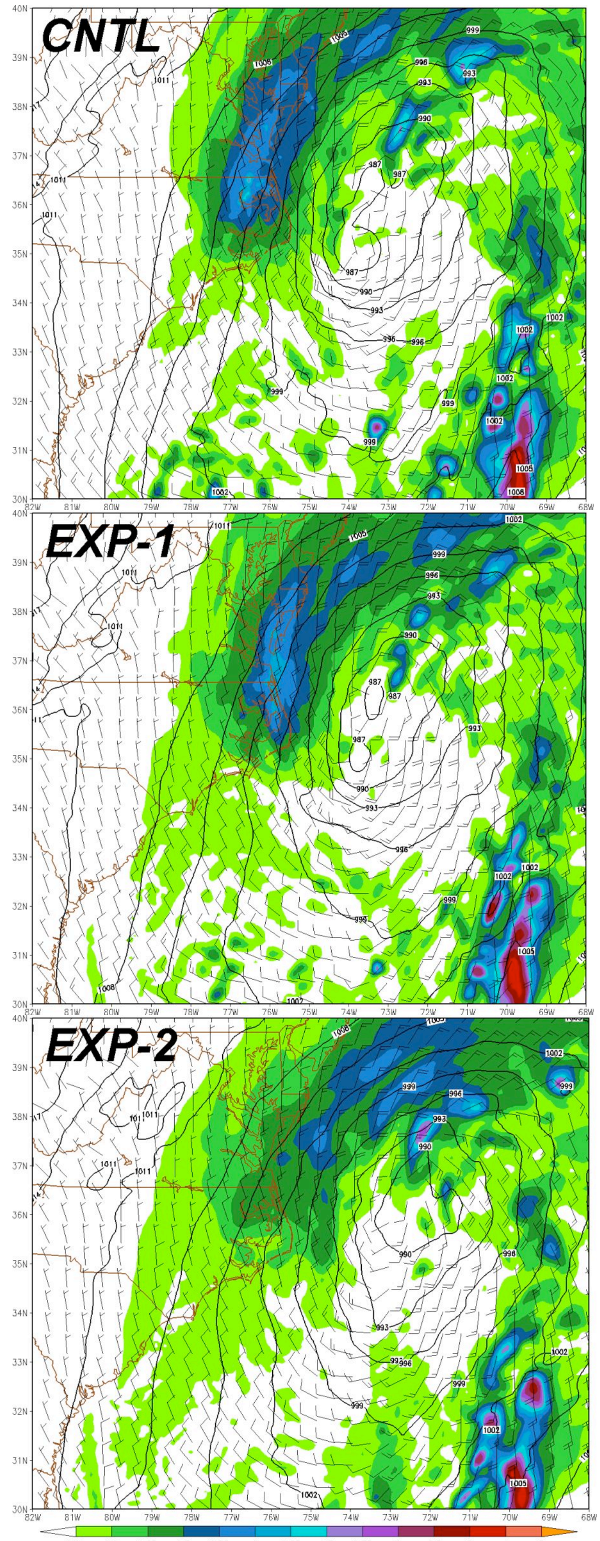

Fig. 6. Sea-level pressure (mb), 10-m winds, and precipitation (in) valid 0900 UTC 25 Jan (33 h into the simulations) for the *Cntl*, *Exp-1*, and *Exp-2*.

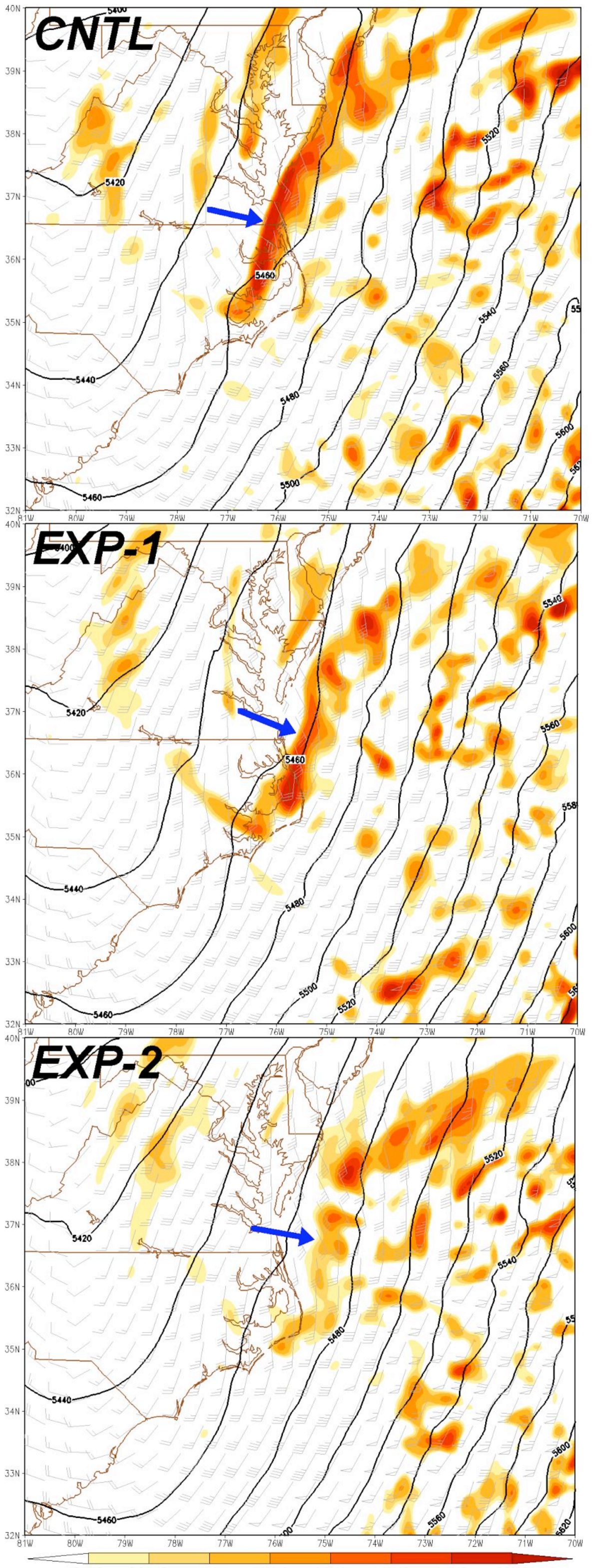

Fig. 7. Simulated 500-hPa heights (m), winds, and divergence (s^{-1}) valid 0900 UTC 25 Jan for the *Cntl*, *Exp-1*, and *Exp-2*.

Exp-1 simulation, and, like the *Cntl*, is following the 291 K isotherm. However, in the *Exp-1* simulation, the 291 K isotherm, as well as the coastal front, is 1° in longitude further to the east. In the *Exp-2* simulation, the coastal front is not well defined. There is still convergence along the 291 K isotherm from 33°N to 36°N, however, north of 36°N, the winds subside. Following the trends of the first two simulations, the coastal front sets up along the 291 K isotherm, which in *Exp-2* is 2.5° east of the *Cntl*.

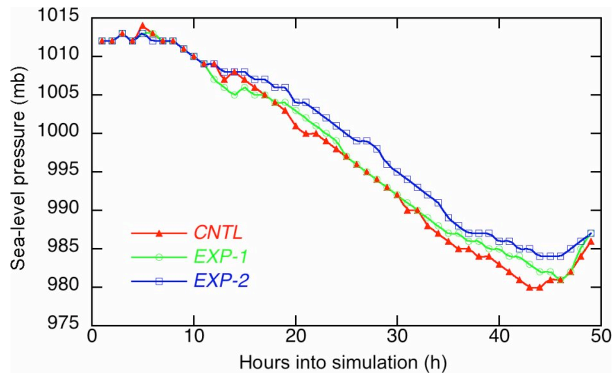

Fig. 8. Time series of the lowest central sea-level pressure for the *Cntl* (red), *Exp-1* (green), and *Exp-2* (blue) simulations. The hours into the simulation run from hour 1 to hour 49, and correspond to 0000 UTC 24 Jan to 0000 UTC 26 Jan.

b) PSBI and ASCII comparison

Calculations for the PSBI, according to the simulations, used the same equation (1) as Part-1. Both T_l = 6°C, and T_{GSF} = 24°C were recorded during the initialization (24 h prior to development), and are the same for the *Cntl*, *Exp-1*, and *Exp-2*. Only Δx, the longitudinal position of the GSF, varies in this experiment. For the *Cntl* simulation, Δx = 78 km, which yields a PSBI value of 2.3°C 10^{-1} km^{-1}. The *Exp-1* Δx = 186 km, which results in a PSBI of 1.0°C 10^{-1} km^{-1}, and the *Exp-2* Δx = 352 km, which results in a PSBI of 0.5°C 10^{-1} km^{-1}. These PSBI values are used below to predict the deepening rate for each of the simulations. The simulated sea-level pressure time series is shown in Fig. 8. Prior to hour 20, the lowest sea-level pressures varied due to localized small-scale features over the GSF. Between hours 20 and 32, the surface low pressure began to rapidly develop. Although the *Cntl* and *Exp-1* have lower pressures than the *Exp-2* simulation, the deepening rates are roughly the same. Between hour 32 and hour 42, the *Cntl* continues to rapidly strengthen, while *Exp-2* slowly strengthens, and *Exp-1* falls in between. Beyond hour 42, all the simulations converge to approximately the same pressure as the storm begins to weaken.

The most rapid decrease in sea-level pressure occurred as the center of the cyclone entered the domain, and was recorded for 12 h. The *Cntl* had a dP/dt = 12mb/12h, *Exp-1* had a dP/dt = 9mb/12h, and *Exp-2* had a dP/dt = 8mb/12h. These values are compared to the deepening rate as predicted by the PSBI in Fig. 9. It is evident that the trends, although linear, do not correlate very well. These results are not particularly surprising since the actual thermal gradient was not changed, just its horizontal location.

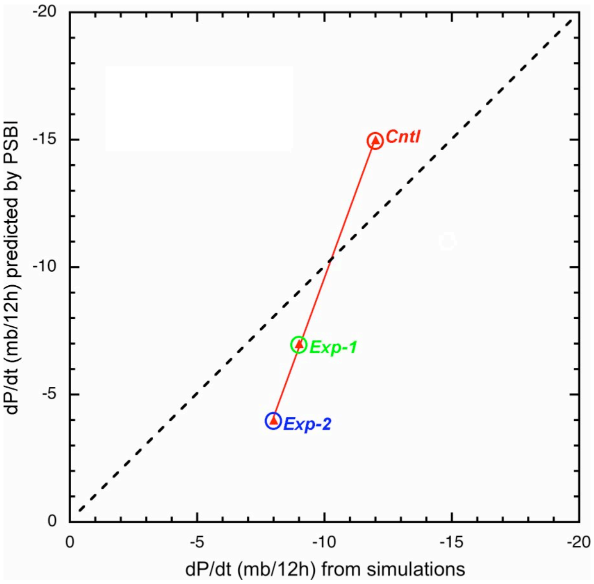

Fig. 9. Comparison between the deepening rate (averaged per 12 h) as predicted by PSBI to the deepening rate simulated by MM5 for *Cntl* (Red), *Exp-1* (green), and *Exp-2* (blue).

8. CONCLUSIONS

As shown by ASCII in Part-1, a weaker thermal gradient will damp low-level cyclogenesis by reducing thermal advection, but in this experiment (Part-2), the gradient was not changed, it was just shifted east by 1° and 2.5° of latitude for the *Exp-1* and *Exp-2* simulations, respectively. Thus, the low-level cyclogenesis in response to the thermal gradient was not significantly reduced, but occurred further east. Pre-existing vorticity along the coastal front, which developed in response to the thermal gradient of the GSF, played a crucial roll in the future track of the surface cyclone. The shift in storm track was likely caused by the horizontal displacement of the coastal front. Since the cyclone will attempt to track along the frontal boundary formed over the GSF as a result of the pre-existing vorticity, by altering the track of the surface low in *Exp-1* and *Exp-2*, the maximum lower-to-upper-tropospheric vertical feedback was reduced, and occurred later, in those respective simulations. This is most noticeable in the plots of precipitation (Fig.6), and the 1-3 h temporal phase shift seen in the time series of sea-level pressure (Fig. 8). The corresponding temporal delays result in the maximum precipitation occurring further north. The lack of deepening in *Exp-2*, as compared to the *Cntl*, is likely a result of the link of vertical feedback to horizontal displacement being too large.

The PSBI comparison illustrates a very important aspect of this experiment, and possibly warrants changing the protocol of horizontal thermal gradient measurements for ASCII. The sensitivity study in Part-2 simulates the opposite extreme from the sensitivity study in Part-1. It would not be particularly realistic to place the GSF over 300 km east of Charleston, SC; however, the objective was to use an extreme event to test how ASCII handles storms at the distribution limits of the climatology regression. In Part-1 of this study, it was shown that by damping the thermal magnitude of the Gulf Stream, the developing coastal low pressure was significantly weakened. This was expected, and the PSBI was in full agreement. The inherent limitation with this method is the inability to separate the reduction in SST from the position of the GSF. Part-2 of this study shifts the location of the Gulf Stream to the east while leaving the SST the same. Since the near-coastal SSTs were extended to the shifted location of the GSF, the actual "thermal gradient" induced by the GSF was not changed, but moved. However, the PSBI measurement is made from land (Wilmington and Cape Hatteras, NC) which, for this case, must span the entire region of extended near-shore SSTs before reaching the GSF, thus making Δx very large over a region where the SST does not change. As expected, the storm rapidly developed over the GSF, albeit further east for each consecutive simulation. In all 3 simulations, there is little difference (<5°C) between the land surface temperatures and the near-shore SSTs. The premise that rapid cyclogenesis occurs over a region where the cold air is advected over warm water with little time to modify still holds true. In Part-2, there was little modification between the coast and the GSF despite the change in distance over which the cold air was advected. This reveals two key aspects: i) The magnitude of the SST of the Gulf Stream exerts a more significant influence on surface cyclogenesis as opposed to the SST gradient[3]. This is concluded from comparing results from Part-1 with those in Part-2. ii) The actual width of the thermal gradient over which the SSTs of the near-shore waters transition to the SSTs of the Gulf Stream, is more important than the distance of the GSF from the shoreline.

The second point leads to the conclusion that Δx (the denominator in the PSBI) may be better suited for the ASCII forecast method if it were a measurement over which only the SST was changing, thus reducing forecast errors for cases where the thermal gradient is tight and the Gulf Stream's SST is high, yet the position of the GSF is far from shore and the near-shore waters have a constant SST.

[3] This can only be stated for the region east of North and South Carolina, and assumes that the coastal land temperatures and near-shore water temperatures are much colder than the maximum SST values of the Gulf Stream (e.g., January, February, etc.), thus the land-based surface temperatures will establish a thermal gradient regardless.

9. ACKNOWLEDGMENTS

The authors are very grateful for the comments and suggestions offered by Dr. Joseph Cione (NOAA, AOML HRD) on this work. The authors would also like to thank Richard Neuherz (NWS Wilmington, NC), Jonathan Blaes (NWS Raleigh, NC), and Kermit Keeter (NWS Raleigh, NC) for their valuable suggestions. The authors are very grateful for the computer support provided by Robert Gilliam (US EPA) and Peter Childs. We would like to thank Dr. Fuqing Zhang (Texas A&M Univ.) for providing the archived Eta-212 GRIB files. This work was supported by the Atmospheric Sciences Division, National Science Foundation under grant # ATM-0342691 and by the State Climate Office of North Carolina.

10. REFERENCES

Bosart, L.F., C. J. Vaudo, and H. J. Helsdon, Jr., 1972: Coastal Frontgenesis. *J. Appl. Meteor.*, **11**, 1236-1258.

Brennan, M. J., and G. M. Lackmann, 2005: The influence of incipient latent heat release on the precipitation distribution of the 24-25 January 2000 U.S. East Coast cyclone. *Mon. Wea. Rev.,* **133**, 1913-1937.

Buizza, R. and P. Chessa, 2002: Prediction of the U.S. Storm of 24-26 January 2000 with the ECMWF Ensemble Prediction System. *Mon. Wea. Rev*., **130**, 1531-1551.

Chen, F., and J. Dudhia, 2001: Coupling an advanced land surface hydrology model with the Penn State/NCAR MM5 modeling system. Part 1: Model description and implementation. *Mon. Wea. Rev* **129**, 569-586.

Cione, J. J., S. Raman, and L. J. Pietrafesa, 1993: The effect of Gulf Stream-induced baroclinicity on the U.S. east coast winter cyclones. *Mon.Wea. Rev.*, **121**, 421-430.

Cione, J. J., S. Raman, R.A. Neuherz, L. J. Pietrafesa, K. Keeter, and Xiaofeng Li, 1998: The Use of Pre-storm Boundary Layer Baroclinicity in Determining and Implementing the Atlantic Surface Cyclone Intensification Index. *Bound.-Layer Meteor.*, **89**, 211-224.

Dudhia, J., 1993: A nonhydrostatic version of the Penn State / NCAR mesoscale model: Validation tests and simulation of an Atlantic cyclone and cold front. *Mon. Wea. Rev*., **121**,1493-1513.

Ek, M. B., K. E. Mitchell, Y. Lin, E. Rogers, P. Grunmann, V. Koren, G. Gayno, and J. D. Tarpley, 2003: Implementation of Noah land-surface model advances in the NCEP operational mesoscale Eta model, *J. of Geophys. Res*., **108**, D22, doi:10.1029/2002JD003296.

Grell, G., 1993: Prognostic evaluation of assumptions used by cumulus parameterizations. *Mon. Wea. Rev*., **121**, 764-787.

Grell, G.A., J. Dudhia, and D.R. Stauffer, June 1994: A Description of the Fifth-Generation Penn State/NCAR Mesoscale Model (MM5), Tech. Rep. NCAR/TN-398+STR, National Center for Atmospheric Research, Boulder, Colorado.

Jacobs, N. A., G. M. Lackmann and S. Raman 2005: The combined effects of Gulf Stream–induced baroclinicity and upper-level vorticity on U.S. East Coast extratropical cyclogenesis. *Mon. Wea. Rev.*, **133**, 2494–2501.

Kalnay, E., M. Kanamitsu, R. Kistler, W. Collins, D. Deaven, L. Gandin, M. Iredell, S. Saha, G. White, J. Woollen, Y. Zhu, M. Chelliah, W. Ebisuzaki, W.Higgins, J. Janowiak, K. C. Mo, C. Ropelewski, J. Wang, A. Leetmaa, R. Reynolds, Roy Jenne, and Dennis Joseph, 1996: The NCEP/NCAR 40-Year Reanalysis Project. *Bull. Amer. Meteor. Soc*., 1996, **77**,437-431.

Kuo, Y.H., and S. Low-Nam, 1990: Prediction of Nine Explosive Cyclones over the Western Atlantic Ocean with a Regional Model. *Mon. Wea. Rev*., **118**, 3-25

Langland, R. H., M. A. Shapiro, and R. Gelaro, 2002: Initial condition sensitivity and error growth in the forecast of the 25 January 2000 east coast snowstorm. *Mon. Wea. Rev*., **130**, 957-974.

Li, X., W. Pichel, P. Clemente-Colon, V. Krasnopolsky, and J. Sapper, 2002: Validation of coastal sea and lake surface temperature measurements derived from NOAA/AVHRR data, *International Journal of Remote Sensing*, **22**, 1285-1303.

NCDC, 2000a: *Storm Data*. Vol. 42, No. 1, 171 pp

Raman, S., and N.C. Reddy , 1996: Numerical simulation of a mesolow over a Gulf Stream filament. Pure and Applied Geophysics, **147**, 789-819.

Sanders, F.J., and J.R. Gyakum, 1980: Synoptic-dynamic climatology of the "bomb". *Mon.Wea. Rev*., **108**, 1589-1606.

Zhang, F., C. Snyder, and R. Rotunno, 2002: Mesoscale Predictability of the “Surprise” Snowstorm of 24-25 January 2000, *Mon. Wea. Rev*., **130**, 1617-1632.